Investigation of Measurement Artifacts Introduced By Horizontal Scanning Surface Profiling Instruments

A Thesis

Submitted to the Faculty

Of

WORCESTER POLYTECHNIC INSTITUTE

In Partial fulfillment of the requirements for the

Degree of Master of Science

in Manufacturing Engineering

by

Torbjorn S. Bergstrom

June 2001

Approval:

Dr. Christopher A. Brown, Major Advisor/Director of Manufacturing Engineering

Abstract

Horizontal scanning instruments, such as, atomic force microscopes and scanning laser microscopes, acquire three-dimensional topographic maps of surfaces, at scales ranging from tenths of nanometers to hundreds of millimeters, by measuring elevations along a series of traces scanning a region of the surface. Random and systematic errors may influence parameters calculated from these topographic maps. This work investigates anisotropic artifacts in atomic force microscope and a scanning laser microscope measurements by looking at difference between parameters calculated in the tracing and scanning directions. It is found that horizontal scanning profiling instruments systematically introduce anisotropic measurement artifacts when measuring both isotropic and anisotropic surfaces.

Table of Contents

List of Figures

Chapter 1 Introduction

1.1. Objective

The objective of this work is to determine if anisotropic measurement artifacts are systematically introduced into measured surfaces by horizontal scanning instruments, which produce three-dimensional topographic maps of surfaces by tracing a series of parallel profiles on an area of the surface.

1.2. Rationale

It is well understood that no measurement system is perfect, and that all measurements contain errors of some kind. It is desirable, therefore, to understand the influence of measurement errors, or artifacts, on the measurements.

Horizontal scanning instruments, such as, atomic force microscopes (AFMs) and scanning laser microscopes (SLMs), acquire three dimensional topographic maps of surfaces, at scales ranging from tenths of nanometers to hundreds of millimeters, by an area profiling method (ASME B46, 1995). Figure 1-1 shows a diagram defining the tracing and scanning directions as discussed in this paper. For the purpose of calculating surface texture parameters, profiles can be formed in either the scanning or tracing direction of the measured surface.

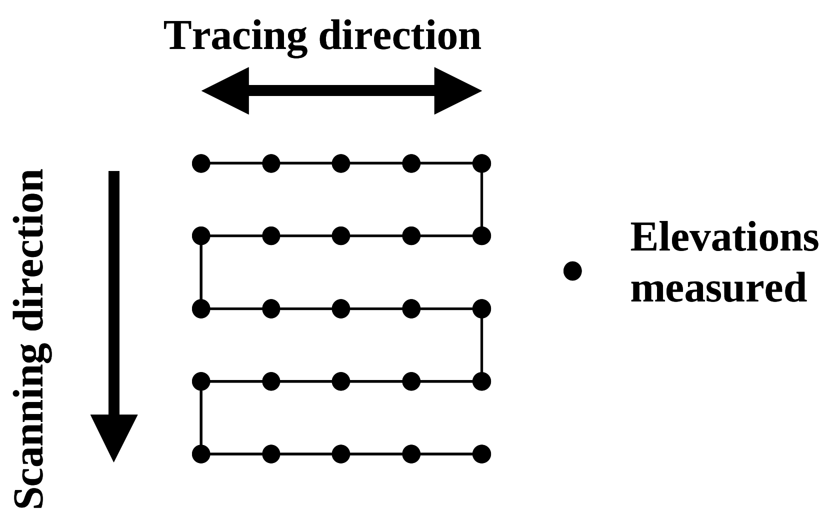

Figure 1-1 Diagram defining the tracing and scanning directions as discussed in this paper. Profiles can be formed in either direction for the purpose calculating surface texture parameters

The measured surface is a representation of the interaction of the measurement instrument and the real surface. Figure 1-2 shows how the SLM measures surfaces by moving the surface under a laser height displacement meter. The SLM used in this study was configured to trace both in the plan of the sensor and perpendicular to the plane of the sensor. The figure shows tracing in the plane of the sensor.

Examination of the SLM shows three obvious means for the introduction of anisotropic artifacts that are related to the method the measurements are made.

1. Difference in noise characteristics of individual positioning tables.
2. The difference in the time delay when comparing adjacent elevations.
3. Asymmetry in the height sensor itself.

The individual positioning tables which position the surface and the height sensor could have different noise characteristics. Even if the differences between the positioning tables were negligible any background noise or building vibrations that are transmitted into the measurement system could cause anisotropic artifacts to be present in the measured surface. Finally the interaction of the laser height sensor with the surface is directional in nature.

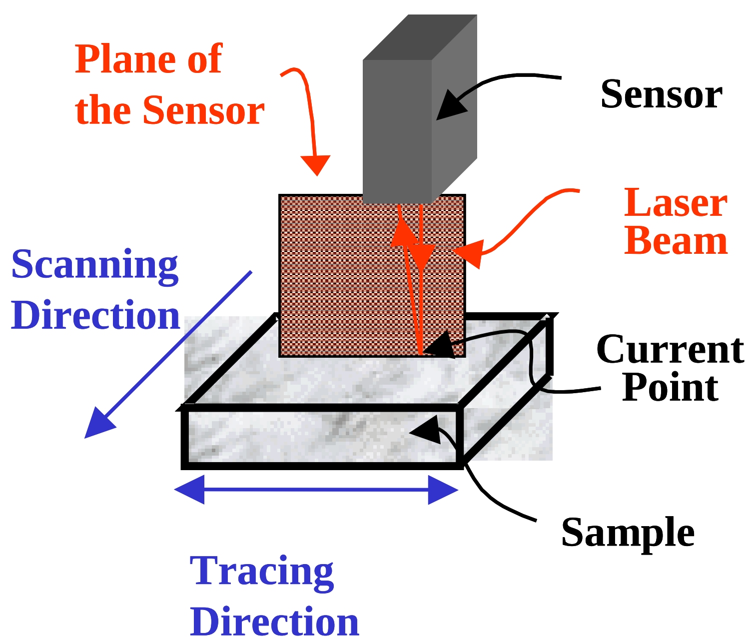

Figure 1-2 Sketch of how SLMs trace and scan surfaces to create a 3 dimensional topographic maps of surfaces.

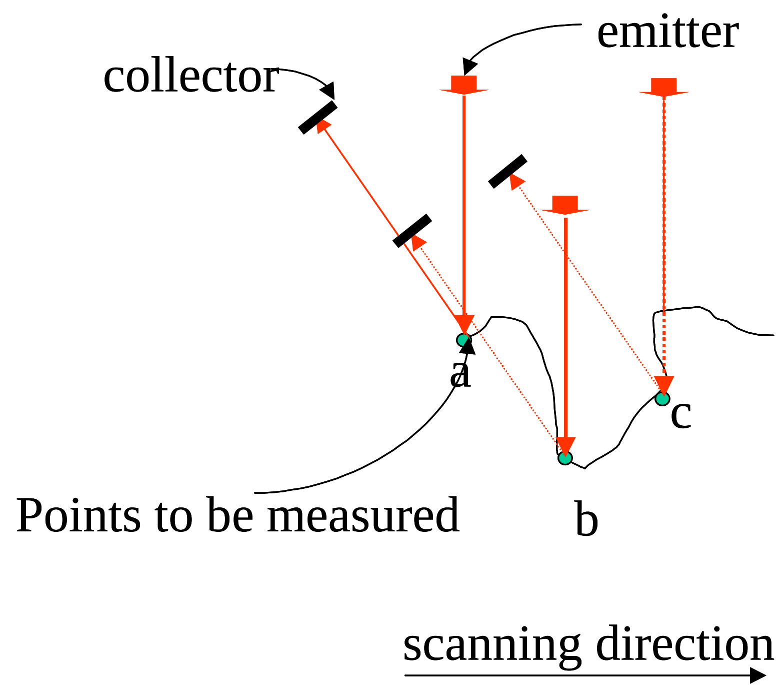

Figure 1-3 Illustration of the interaction of the laser beam with the surface. Points b and c cannot be measured by the sensor in this orientation.

Figure 1-3 shows that the sensor cannot see some points in deep valleys or points "shadowed" by overhangs. This means that the orientation of the surface relative to the plane of the sensor can be critical in the measurement of surface topography. The SLM used in this study has a single light detector. Alternate sensors could be used on an SLM that offer multiple light detectors, even a ring of detectors could be used but you would still be similarly limited by some ratio of the depth to diameter ratio of any "depressions" in the surface.

Sources of error discussed above are inherent to horizontal scanning profiling instruments. AFMs interact with surfaces similarly to SLMs (see Figure 1-4). With AFMs there is not the problem of the bottom of valleys being in the shadow of adjacent peaks, but tip geometries however are asymmetric and could conceivably introduce anisotropy into the measurement at some scale.

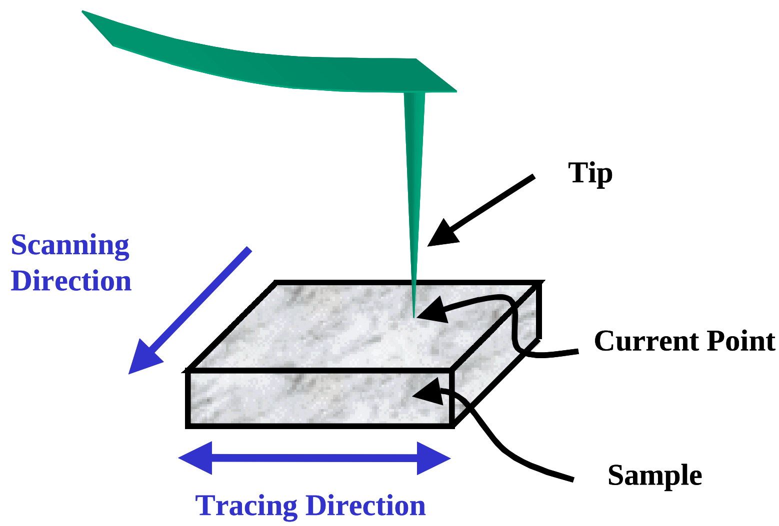

Figure 1-4 Sketch of how AFMs trace and scan surfaces to create a 3 dimensional topographic maps of surfaces.

1.3. State-of-the-art

Nothing was found in the literature to indicate that the introduction of anisotropy into measured surfaces by horizontal scanning instruments has been considered in the past.

The characterization of anisotropy in rough surfaces has been studied. (Thomas 1999, Bush et. al. 1979, Russ 1994).

1.4. Approach

In this work surfaces are measured with three horizontal scanning instruments, two Digital Instruments Nanoscope™ III AFMs, and a scanning laser microscope built in the Surface Metrology Laboratory at WPI for measuring runway surface textures in a project with NASA Langley Research center. The measured surfaces were analyzed using conventional surface texture parameters (ASME B46.1-1995) and scale sensitive fractal parameters (Brown et. al. 1991).

Chapter 2 of the thesis will discuss the measurements made with the two AFMs, and the analysis of these measurements. It is concluded that measurements of both isotropic and anisotropic surfaces contain measurement artifacts which depending on the circumstances of the measurement could add to or mask any anisotropy in the real surface. The sensitivity of the different surface texture parameters calculated to these measurement artifacts is also discussed.

In Chapter 3 a similar study using the SLM is presented. This study is limited to the scale sensitive fractal parameters, as these parameters proved more sensitive to the anisotropic artifacts studied in Chapter 2. In Chapter 3, it was found that conclusions of Chapter 2 held true for this instrument also.

Chapter 4 presents and discusses a method for determining the scale ranges the instruments are introducing anisotropic artifacts into the measured surfaces. The method is applied to one set of the AFM measurements presented in Chapter 2 as an example.

Chapter 2 AFM

2.1. Introduction

2.1.1. Objective

The objective of this chapter is to determine if anisotropic measurement artifacts are systematically introduced into measured surfaces by Atomic Force Microscopes, and to investigate surface texture parameters that can be affected by these artifacts.

2.1.2. Rationale

It is important to understand the capabilities and limitations of equipment we use. It has been shown that functional correlations can be made between surface texture parameters and surface behavior characteristics (Siegmann and Brown, 2001). It is possible that small differences in the actual surface texture could be very important in determining whether a manufactured part will function correctly. If isotropy is desired for example and anisotropy is found in the measured surface due to measurement artifacts it may be possible to modify a manufacturing process to remove the apparent anisotropy while in fact adding anisotropy to the real surface.

2.1.3. State-of-the-art

Studies on determining the anisotropy of rough surfaces have been completed using computer-generated models of surfaces, and using measured surfaces acquired by atomic force microscopes (Grigoriv et. al. 1997).

There was no reference found in the literature about the possibility of anisotropic measurement artifacts, which could be introduced into the measured surfaces acquired by AFMs.

Approach

The approach of this study is to look at conventional and area-scale fractal parameters calculated from measured surfaces acquired from apparently isotropic surfaces and anisotropic surfaces to determine if measurement artifacts are masking or adding to the anisotropy of these measured surfaces.

Two surfaces were studied, one that appeared isotropic on visual inspection, and another that was strongly anisotropic (Russ 1994). On the strongly anisotropic surface, known anisotropic features of the surface or controlled for by only comparing analyses calculated along the same direction of the surface.

2.2. Methods

This study can be broken up into two basic parts, the acquisition of the measured surfaces and the analysis of the measured surfaces. Measured surfaces acquired with two Digital Instruments Nanoscope III Atomic Force Microscopes (AFMs) are examined. Measurements were made on a piece of diamond coated silicon substrate and a contact lens. The measured surfaces were analyzed using conventional profile surface texture parameters, and scale-sensitive fractal analysis. The analyses were done for the areas measured, and along the profiles formed by extracting the rows and columns from the measured surfaces.

This section of the report will describe the methods for the measurement or acquisition of the measured surfaces and the methods for the analysis of the measured surfaces.

2.2.1. Measurement

For the AFMs used it is possible to vary a number of measurement parameters. This study varied the direction of tracing relative to the tip orientation and relative to the orientation of the surfaces.

The preliminary study was done using an apparently isotropic surface. Measurements were made at two locations on the surface with various angles between the tracing direction and the tip orientation. Further study was done by measuring a contact lens that had been intentionally scratched making it strongly anisotropic (Russ, 1994). Tracing both perpendicular to and parallel to the scratch then rotating the surface 90 degrees and repeating this process controlled for the isotropic nature of this surface. The sections below describe in detail the steps in acquiring the measured surfaces to be analyzed.

2.2.1.1. Apparently Isotropic Surface

The first surface measured was a piece of diamond coated silicone substrate. Visual inspection with an optical microscope showed the surface to be isotropic. The estimated diamond grain diameter was between 5 to 8 μm. Figure 2-1 shows a typical 20 μm by 20 μm area on the surface.

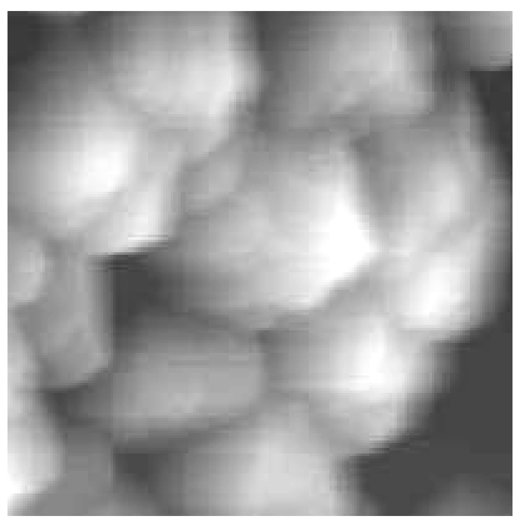

Figure 2-1 20μm by 20μm image if diamond coated silicon substrate.

All measurements of the diamond coated silicon substrate were made with a Digital Instruments Nanoscope III ™ AFM. The AFM was set for non-contact mode and two Si_3N_4 tips were used. Measurements, made with a broken tip, were discarded. The measurement settings are listed in Table 2-1 below.

Table 2-1 Settings for measurements of diamond coated silicone substrate.

Length of trace	100 μm
Number of traces	512
Distance between traces	0.1953125 μm
Area measured	100 by 100 μm
Elevations per trace	512
Direction of trace relative to cantilever	See Table 2-2

A total of seven measurements were made at two different locations on the surface. All of the measurements were made with the specimen in the same orientation. The tracing direction relative to the orientation of the AFM tip was varied. Table 2-2 shows the location and tracing directions of the measured surfaces from the diamond coated silicone substrate. An angle of 0° is parallel to the cantilever.

Table 2-2 Measurment locations and tracing directions on diamond coated silicon substrate.

Measurement	Location	Trace Direction Relative to Cantilever
1-1	1	10°
1-2	1	100°
1-3	1	190°
1-4	1	190°
2-1	2	0°
2-2	2	0°
2-3	2	90°

Figure 2-2 illustrates the information in Table 2-2. The arrows indicate the tracing direction, with double ended arrow indicating retrace the retrace option was selected. The cantilever orientation is vertical relative to the page.

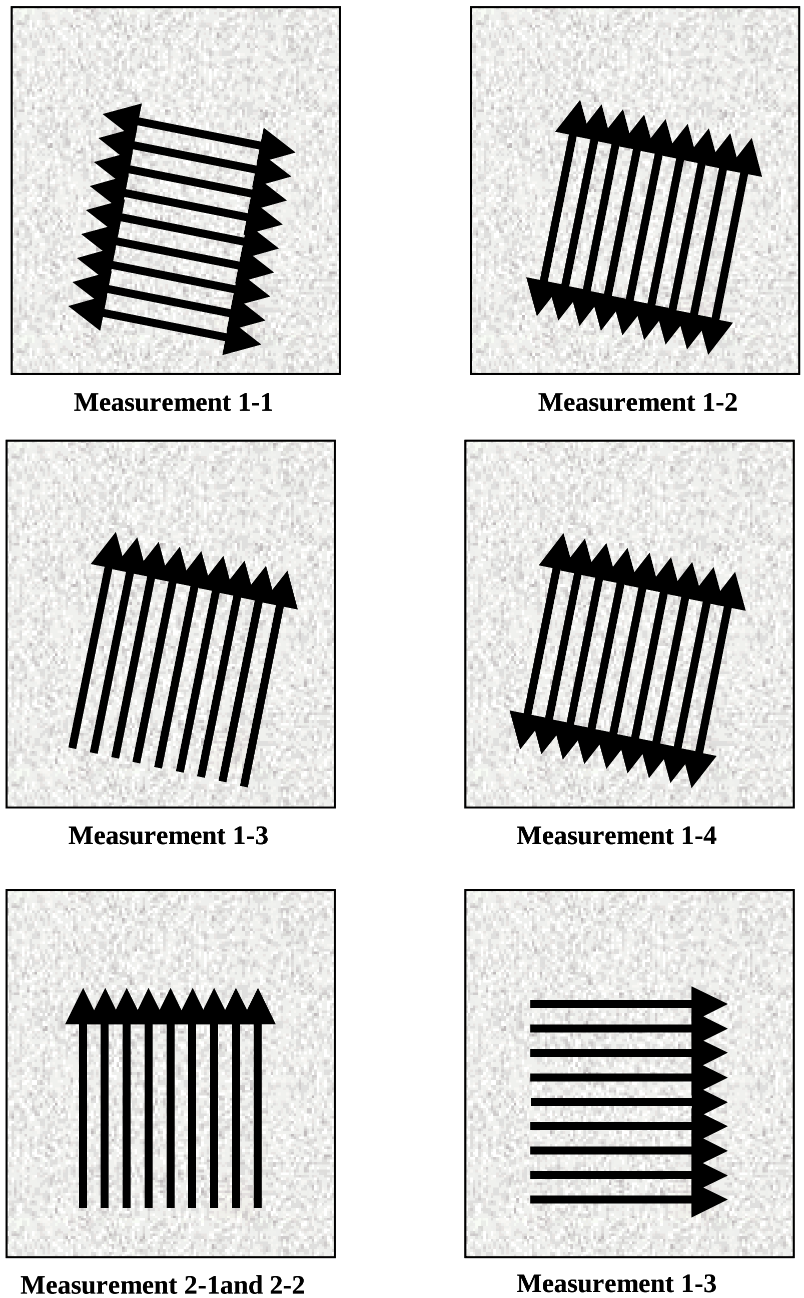

Figure 2-2 Sketch showing measurement locations and tracing directions for measurements of diamond coated silicone substrate.

2.2.1.2. Apparently anisotropic surface

Additionally a surface that was intentionally scratched, making it strongly anisotropic (Russ, 1994), was measured. The surface was a Bausch and Lomb Pure Vision ™ contact lens. These measurements were also made with a Digital Instruments Nanoscope III ™ AFM. Table 2-3 shows the settings for the measurements made on the contact lens. In this case a single tip was used.

Table 2-3 Settings for measurements of diamond coated silicone substrate.

Length of trace	50 μm
Number of traces	512
Distance between traces	0.09765625 μm
Area measured	50 by 50 μm
Elevations per trace	512
Direction of trace relative to cantilever	0° or 90° (see below)

Measurements were made at three locations on the lens. At each location the surface was measured by tracing parallel to the cantilever (0°) and perpendicular to the cantilever (90°). The surface was then rotated 90° and the 0° and 90° measurements were repeated. A total of 12 measurements were made.

2.2.2. Analyses

The same analyses were applied to all of the measurements from both surfaces. Four analysis techniques were utilized. Conventional area and profile amplitude type surface texture parameters and area and profile fractal parameters were calculated. For the profile type parameters calculations were made parallel to and perpendicular to the tracing direction.

On this strongly anisotropic surface, the anisotropy of the surface was controlled for by only comparing analyses made in the same direction relative to the surface orientation.

2.2.2.1. Conventional Analysis

The conventional surface parameters were calculated per the definitions provided in ASME B46.1-1995. No filtering was applied to the measurements, and no cutoff values were used, so the parameters calculated utilized all of the measured elevations. For the profile parameters calculated each profile was individually leveled and normalized along the direction of the analysis. The parameters were calculated for each profile in the measurement and averaged to give a single value for each parameter for each measurement. Table 2-4 shows a list of the conventional parameters calculated.

Table 2-4 Conventional surface parameters calculated (ASME B46.1-1995).

Profile Parameters	Area Parameters
Pt	APt
Pa	APa
Pt	APt
Pq	APq

2.2.2.2. Fractal Analysis

Table 2-5 shows the fractal parameters calculated. Figure 2-4, an annotated length scale plot illustrates how each parameter is calculated.

Table 2-5 Fractal surface parameters calculated.

Profile Parameters		Area Parameters
Parallel to Tracing Direction	Perpendicular to Tracing Direction	
Lsfc	Lsfc	Asfc
SRC	SRC	SRC
Dls	Dls	Das

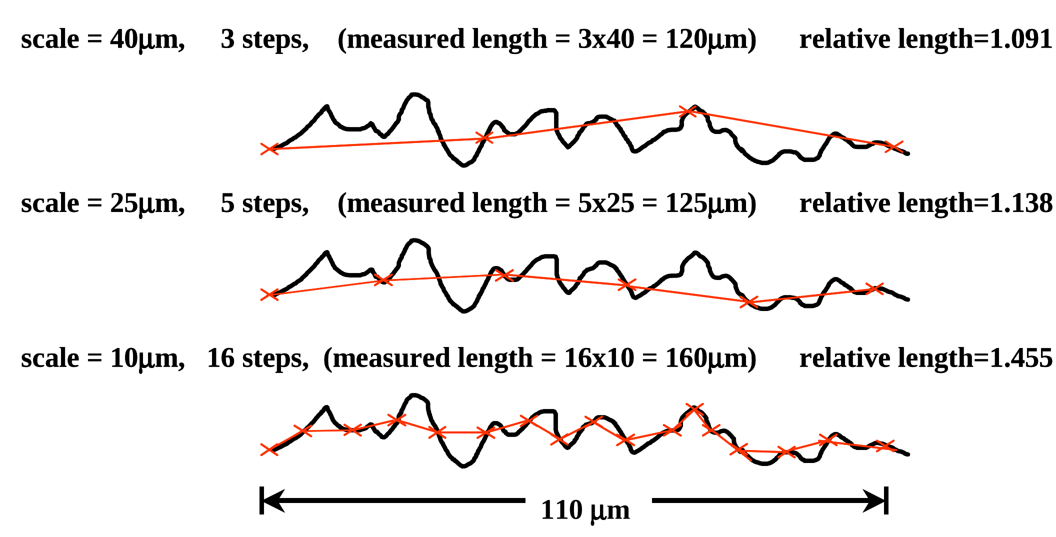

Figure 2-3 Length-scale tiling diagram.

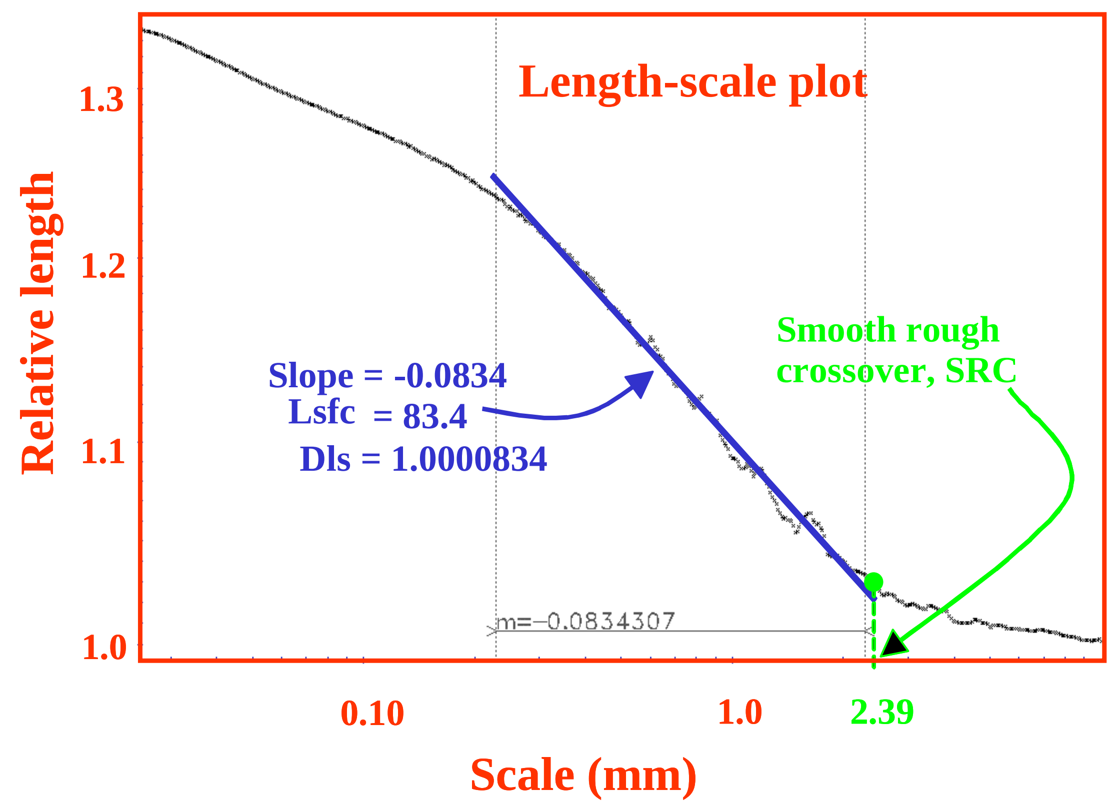

Figure 2-4 Annotated length scale plot.

Length-scale analysis is a type of fractal analysis based on the Richardson, coastline or compass method. The method analyzes the changes in the relative length (ratio of the measured length to the straight-line length) of a profile, which increases as the scale of measurement decreases (Figure 2-3). Three parameters are derived from the analysis. The length-scale fractal complexity, Lsfc, is negative 1000 times the slope of a regression line fit to a portion of the log-log, length-scale plot (Figure 2-4). The Lsfc is related to the fractal dimension (Dls = 1 + (Lsfc/1000)). The smooth-rough crossover, SRC, is the scale that delineates the coarse scale regions where the profile appears smooth, or Euclidean, from the fine scale regions where it appears rough, or fractal. At scales below the SRC the relative lengths are significantly greater than one. These parameters, unlike average roughness, depend on the order of the measured heights in the profiles. The complexity and crossover are orthogonal measurements, in that one can change without influencing the other.

The area fractal parameters are similarly determined using a log-log plot of relative area verses scale instead of relative length. The relative area is determined by covering the measured surface with various sized triangular tiles and dividing the total surface area of the triangular tiles at a given scale by the projected area of those tiles on the best fit plane through the surface. For a given scale all of the triangular tiles maintain the same area, but are allowed to vary in shape within some limits.

For an isotropic surface the fractal dimension of any profile through the surface will be equal to the surface fractal dimension (Dls = Das-1) (Russ 1994).

2.3. *Results*

2.3.1. Isotropic Surface

In this section of the report the results of the study on the AFMs are reported. First the AFM images are presented for the isotropic sample (the diamond coated silicon substrate). Then the results for the conventional analysis are presented followed by the results of the fractal analysis of these measurements. Next the AFM images of the anisotropic sample (the scratched contact lens) are presented likewise followed by the conventional and fractal analyses of these measurements.

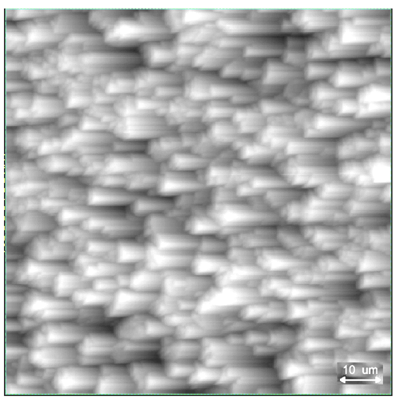

Measurement 1-1

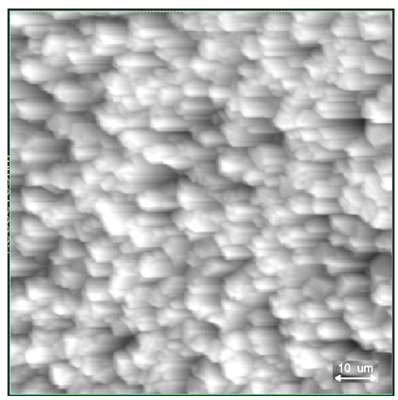

Measurement 1-2

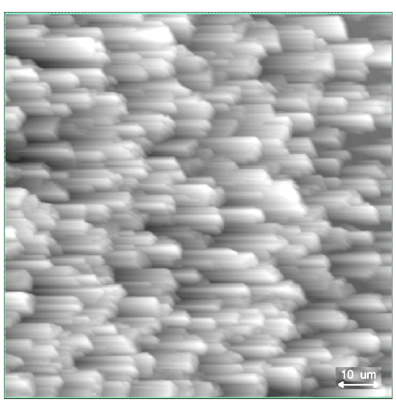

Measurement 1-3

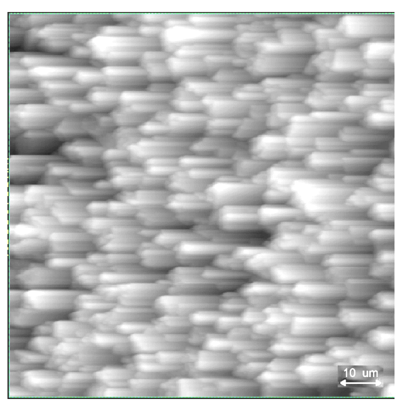

Measurement 1-4

Figure 2-5 AFM images of diamond coated silicone substrate. Measurements made at location 1 on the surface, all traced off axis from the direction of the cantilever (see Table 2-2).

Figure 2-5 shows the images or top down view of the AFM measurements at location one on the diamond coated silicon substrate. These measurements were all traced off axis from the direction of the cantilever (see Table 2-2). Figure 2-6 shows the AFM images of the measurements at location 2 on the diamond coated silicon substrate. The two measurements shown on the right were traced parallel to the direction of the cantilever. The measurement shown on the left was made tracing perpendicular to the cantilever.

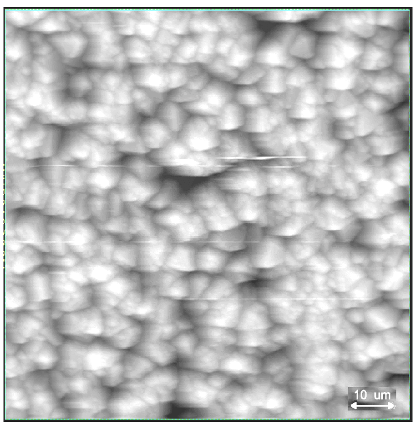

Measurement 2-1

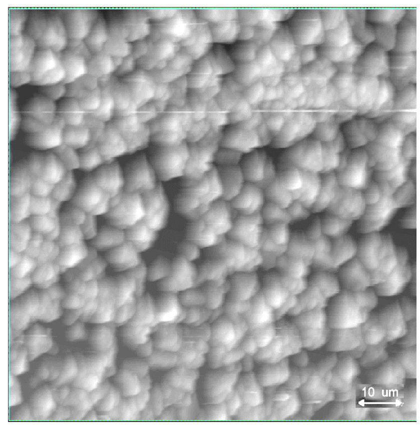

Measurement 1-3

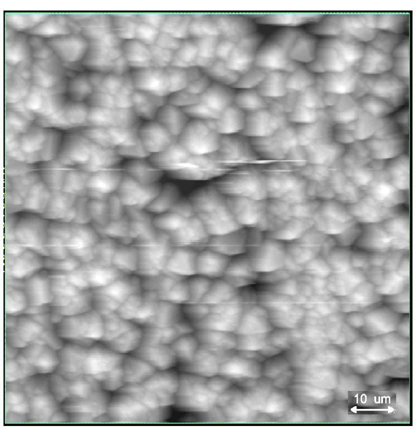

Measurement 2-2

Figure 2-6 AFM images of location 2 on diamond coated silicon substrate, all traced perpendicular or parallel to the direction of the cantilever.

2.3.1.1. Conventional Analysis

Table 2-6 shows the results of the conventional analysis of the AFM measurements of the diamond coated silicon substrate.

Table 2-6 Conventional profile parameters calculated conventional for diamond coated silicon substrate measurements.

	Analysis parallel to the tracing direction				Analysis perpendicular to the tracing direction			
Measurement	Ra (μm)	Rq (μm)	Rp (μm)	Rt (μm)	Ra (μm)	Rq (μm)	Rp (μm)	Rt (μm)
1-1	0.300	5.156	157.019	324.499	0.299	5.138	159.224	340.570
1-2	0.304	5.241	162.253	327.917	0.323	5.589	170.407	361.180
1-3	0.287	4.959	156.064	307.136	0.306	5.331	170.113	358.317
1-4	0.283	4.862	153.844	296.232	0.297	5.087	166.796	327.856
2-1	0.280	4.881	136.554	311.328	0.276	4.802	156.931	343.268
2-2	0.301	5.216	148.394	329.732	0.297	5.154	175.536	367.966
2-3	0.276	4.730	153.497	297.439	0.288	4.971	158.806	318.580

Figure 2-7 shows a graphical representation of the results for the conventional profile analysis. The black filled bars in each plot represent the analysis was perpendicular to the tracing direction, while the gray filled bars are for the analysis parallel to the tracing direction.

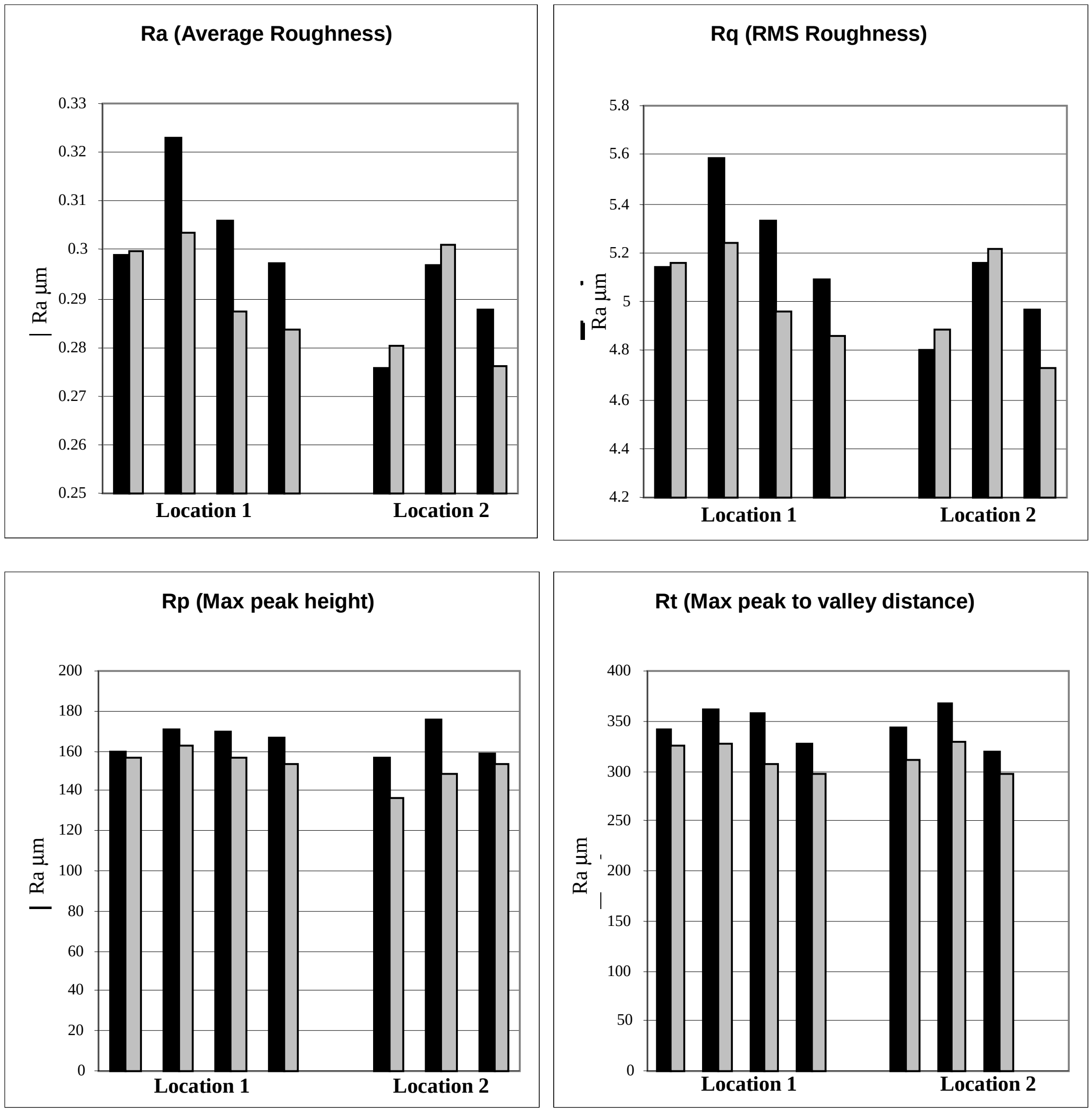

Figure 2-7 Results of conventional profile analysis of diamond coated silicon substrate.

In each plot in Figure 2-7 the gray bars indicate that the analysis was along the tracing direction and the black bars indicate the analysis was along the scanning direction.

2.3.1.2. Fractal Analysis

Area and length scale fractal parameters were calculated for all of the measurements, see Table 2-5, Comparison of the area and profile fractal dimensions is a good indicator of weather a surface is isotropic (Thomas, 1999). Following are the results for the fractal analysis for the diamond coated silicone substrate.

Table 2-7 shows the area parameters calculated, Table 2-8 lists the length scale parameters calculated, and Table 2-9 the area and length scale fractal dimensions for all of the measurements. Figure 2-8 is a plot showing the SRC versus the Length scale complexity for all of the measurements.

Table 2-7 Fractal area parameters calculated for diamond coated silicon substrate measurements.

Measurement	SRC (μm^2)	ASFC	Area Fractal Dimension
1-1	17.98	0.46	2.00046
1-2	19.19	0.41	2.00041
1-3	14.56	0.50	2.00050
1-4	14.56	0.51	2.00051
2-1	13.50	0.44	2.00044
2-2	14.56	0.44	2.00044
2-3	17.98	0.37	2.00037

Table 2-8 Fractal profile parameters calculated for diamond coated silicon substrate measurements.

Measurement	Parallel SRC (μm)	Parallel LSFC	Parallel Fractal Dimension	Perpendicular SRC (μm)	Perpendicular LSFC	Perpendicular Fractal Dimension
1-1	7.49	0.31	1.00031	4.98	0.67	1.00067
1-2	8.81	0.20	1.00020	5.56	0.64	1.00064
1-3	10.86	0.15	1.00015	4.51	0.86	1.00086
1-4	7.82	0.23	1.00023	4.39	0.84	1.00084
2-1	8.32	0.23	1.00023	3.96	0.84	1.00084
2-2	8.21	0.26	1.00026	4.39	0.84	1.00084
2-3	6.16	0.40	1.00040	5.04	0.56	1.00056

Table 2-9 Area and profile fractal dimensions for diamond coated silicon substrate measurements.

Measurement	Area Fractal Dimension	Parallel Fractal Dimension	Perpendicular Fractal Dimension
1-1	2.00046	1.00031	1.00067
1-2	2.00041	1.00020	1.00064
1-3	2.00050	1.00015	1.00086
1-4	2.00051	1.00023	1.00084
2-1	2.00044	1.00023	1.00084
2-2	2.00044	1.00026	1.00084
2-3	2.00037	1.00040	1.00056

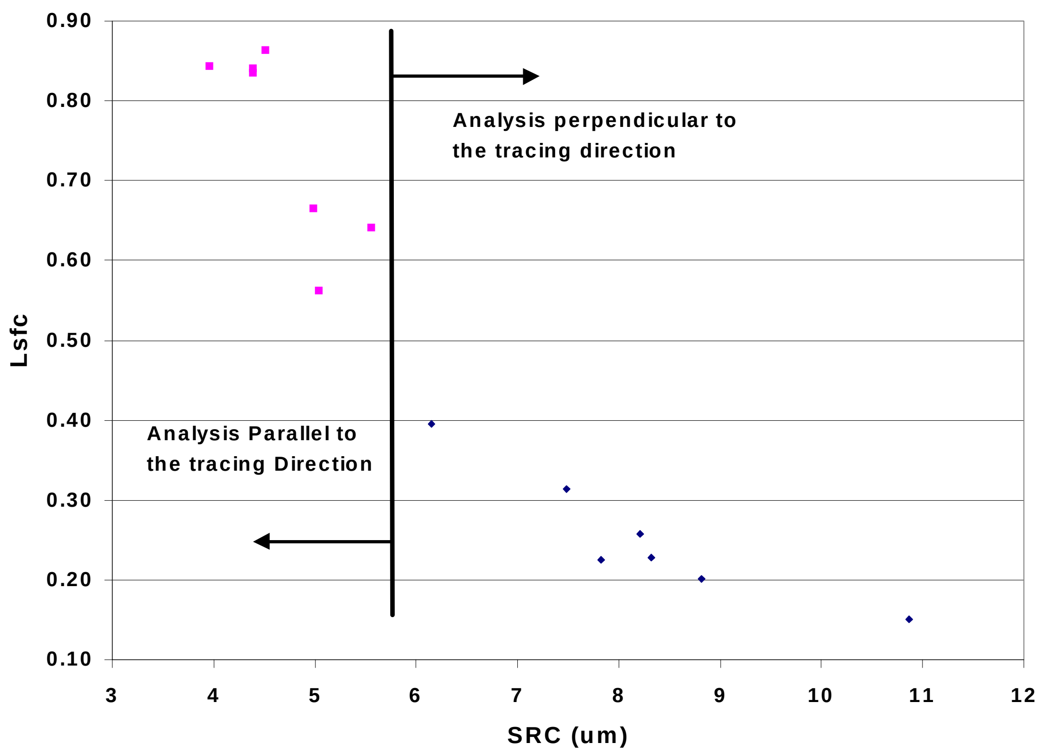

Figure 2-8 Length scale complexity vs smooth rough crossover for measurments at locations 1 and 2 on diamond coated silicon substrate

2.3.2. Anisotropic Surface

Figure 2-9 shows typical AFM images of the measurements performed n the contact lens. The scratch on the lens is clearly visible in all of the images. Each image is 50 μm by 50 μm with 512 measured points in both the tracing and scanning directions. On each measured surface there is a row of “bumps” diagonal to the scratch and also a less deep scratch parallel the scratch made for location purposes. It is un-clear if these are actual surface features, or are measurement artifacts

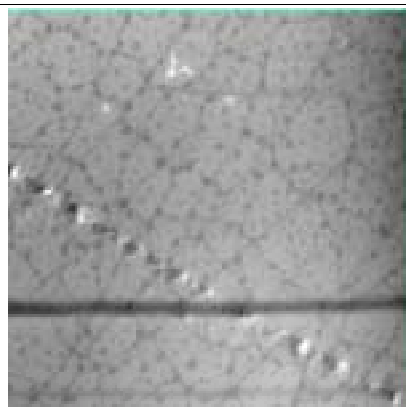

a. First orientation traced parallel

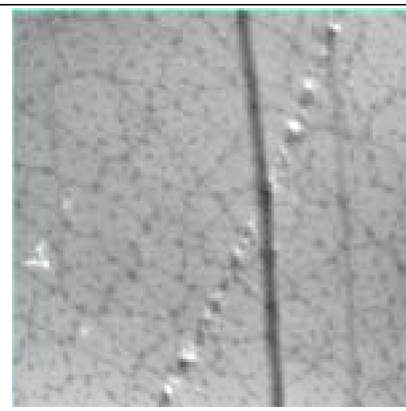

b. First orientation traced perpendicular

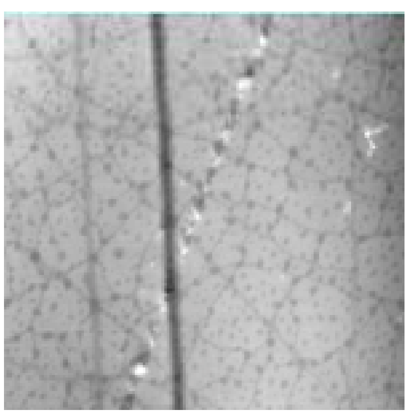

c. Second orientation traced parallel

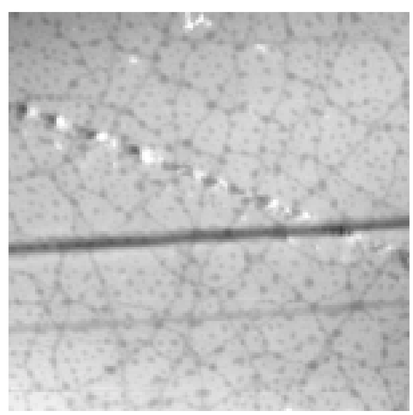

d. Second orientation traced perpendicular

Figure 2-9 Typical 50μm x 50μm AFM images of contact lens. The scratch intentionally made for location purposes is clearly visible.

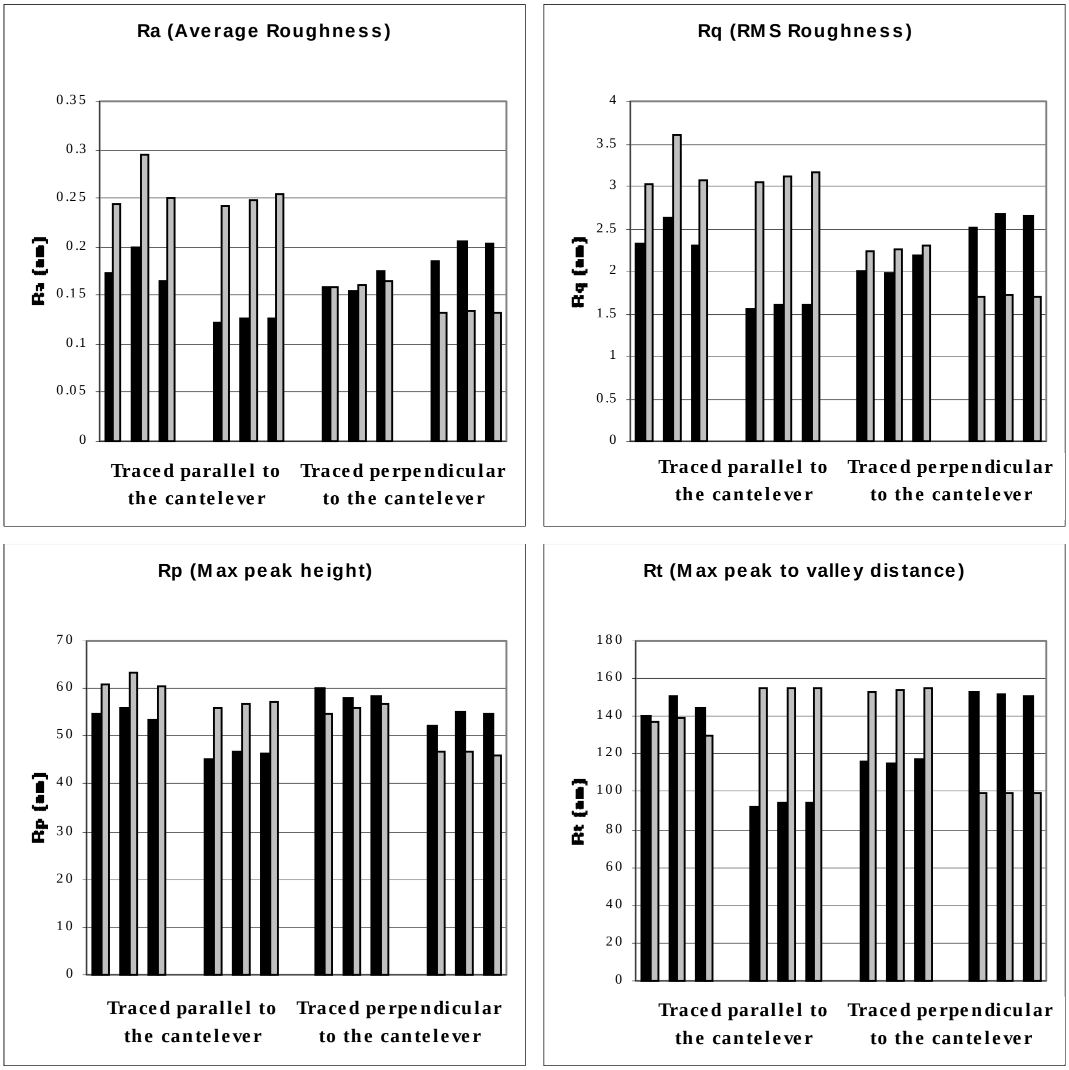

Figure 2-10 Results of conventional profile analysis on contact lens.

2.3.2.1. Conventional analysis.

Table 2-11 shows the results of the conventional analysis of the AFM measurements of the contact lens. Figure 2-10 shows a graphical representation of the results for the profile analysis.

As with the plots of conventional parameters from the measurements of the diamond coated substrate (Figure 2-7) the gray bars in all of the plots in indicate the analysis was along the tracing direction and the black bars indicate the analysis was along the scanning direction. In Figure 2-10 the analysis direction relative to the cantilever orientation is also indicated on the plots.

2.3.2.2. Fractal Analysis

Table 2-11 lists the profile fractal parameters for these measurements. Figure 2-11 shows the length scale and smooth rough crossovers plotted versus complexity.

Table 2-11 Fractal profile parameters calculated for contact lens measurements.

orientation 1 traced parallel to the cantilever						
	Analysis Parallel to the tracing direction			Analysis perpendicular to the tracing direction		
	SRC (μm)	Lsfc	Fractal Dimension	SRC (μm)	Lsfc	Fractal Dimension
location 1	1.60	0.39	1.00039	2.50	0.35	1.00035
location 2	1.60	0.37	1.00037	2.30	0.36	1.00036
location 3	1.50	0.36	1.00036	2.50	0.35	1.00035
orientation 2 traced parallel to the cantilever						
	Analysis Parallel to the tracing direction			Analysis perpendicular to the tracing direction		
	SRC (μm)	Lsfc	Fractal Dimension	SRC (μm)	Lsfc	Fractal Dimension
location 1	2.00	0.40	1.00040	1.50	0.28	1.00028
location 2	2.00	0.40	1.00040	1.50	0.29	1.00029
location 3	2.20	0.41	1.00041	1.50	0.28	1.00028
orientation 1 traced perpendicular to the cantilever						
	Analysis Parallel to the tracing direction			Analysis perpendicular to the tracing direction		
	SRC (μm)	Lsfc	Fractal Dimension	SRC (μm)	Lsfc	Fractal Dimension
location 1	1.60	0.33	1.00033	1.60	0.37	1.00037
location 2	1.60	0.32	1.00032	1.50	0.37	1.00037
location 3	1.50	0.33	1.00033	1.50	0.38	1.00038
orientation 2 traced perpendicular to the cantilever						
	Analysis Parallel to the tracing direction			Analysis perpendicular to the tracing direction		
	SRC (μm)	Lsfc	Fractal Dimension	SRC (μm)	Lsfc	Fractal Dimension
location 1	2.20	0.40	1.00040	2.10	0.40	1.00040
location 2	2.20	0.39	1.00039	2.10	0.39	1.00039
location 3	2.24	0.41	1.00041	2.20	0.38	1.00038

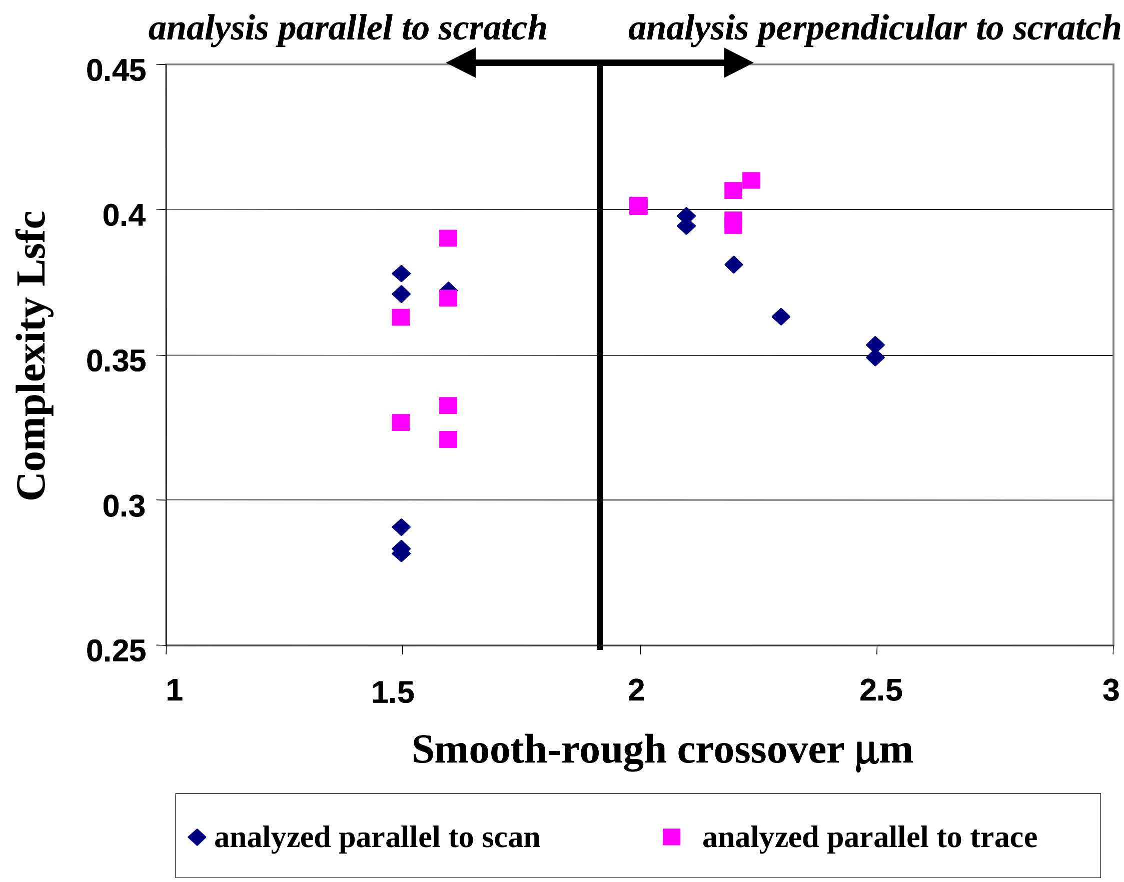

Figure 2-11 Length scale complexity vs smooth rough crossover for all analysis on contact lens

Figure 2-11shows the SRC vs Lsfc for all of the analysis. Figure 2-12, Figure 2-13, Figure 2-14, and Figure 2-15 show the SRC vs Lsfc for each set of analysis either perpendicular or parallel to the scratch for each tracing direction relative to the cantilever orientation.

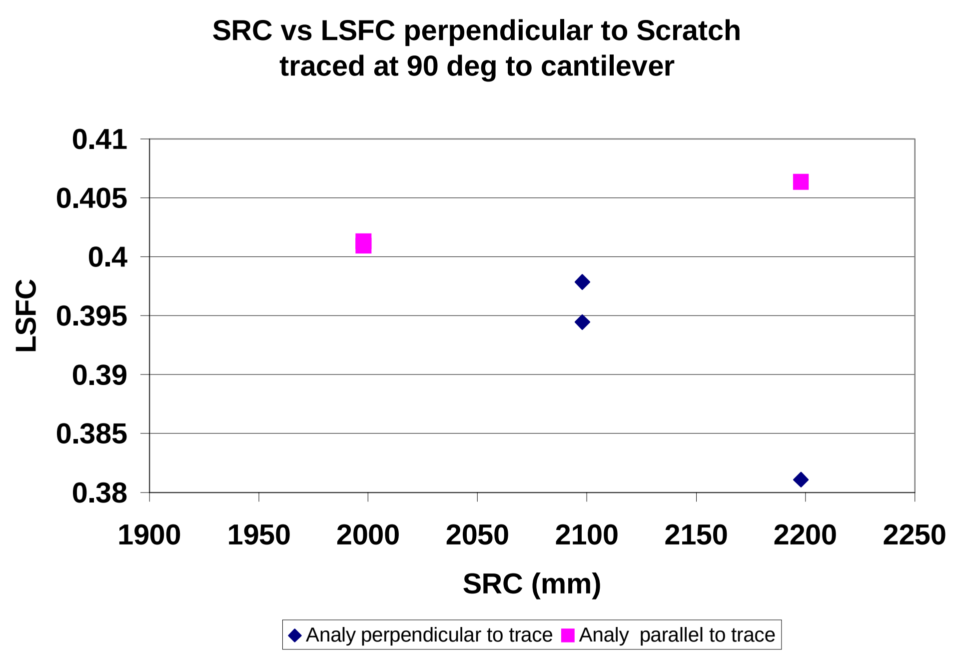

Figure 2-12 Length scale complexity vs smooth rough crossover for analysis perpendicular to the scratch traced at 90 deg relative to the cantilever on contact lens

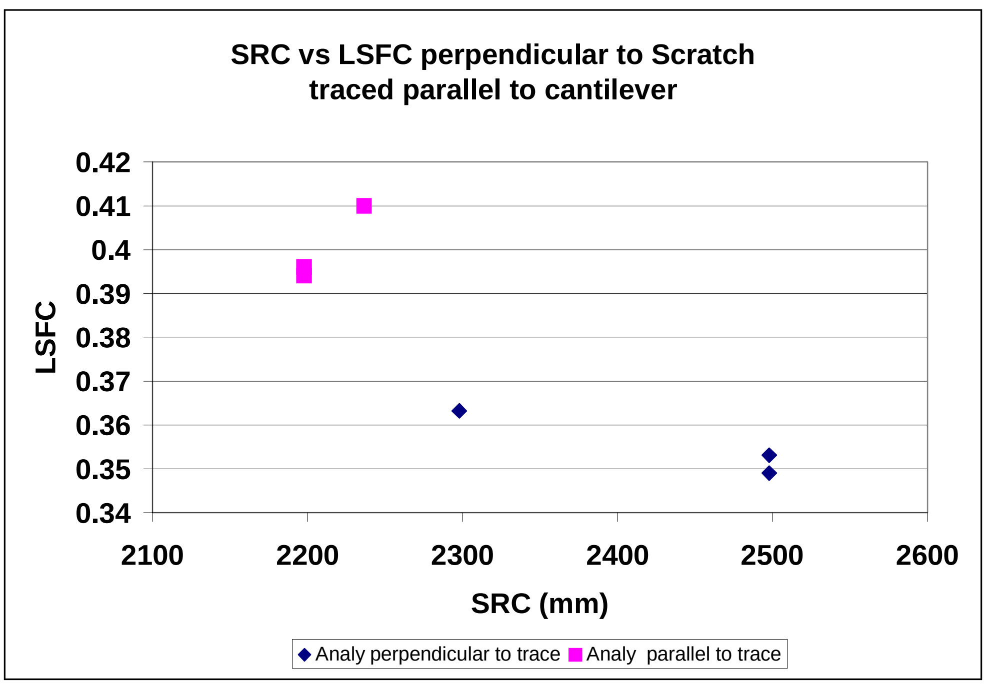

Figure 2-13 Length scale complexity vs smooth rough crossover for analysis perpendicular to the scratch traced at 0 deg relative to the cantilever on contact lens

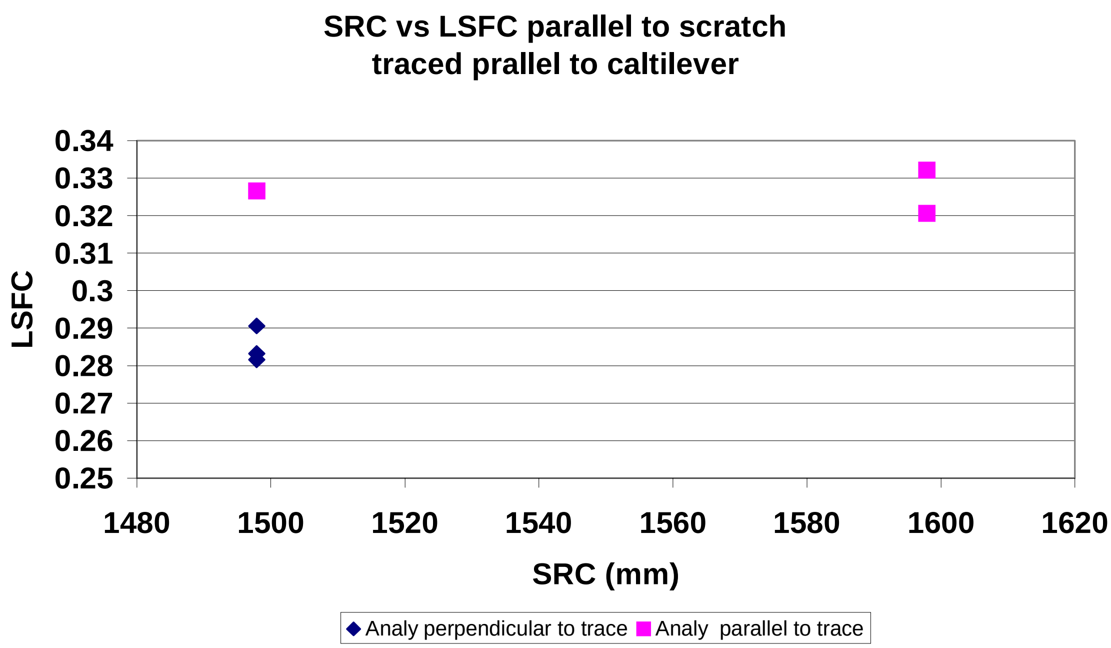

Figure 2-14 Length scale complexity vs smooth rough crossover for analysis parallel to the scratch traced at 0 deg relative to the cantilever on contact lens

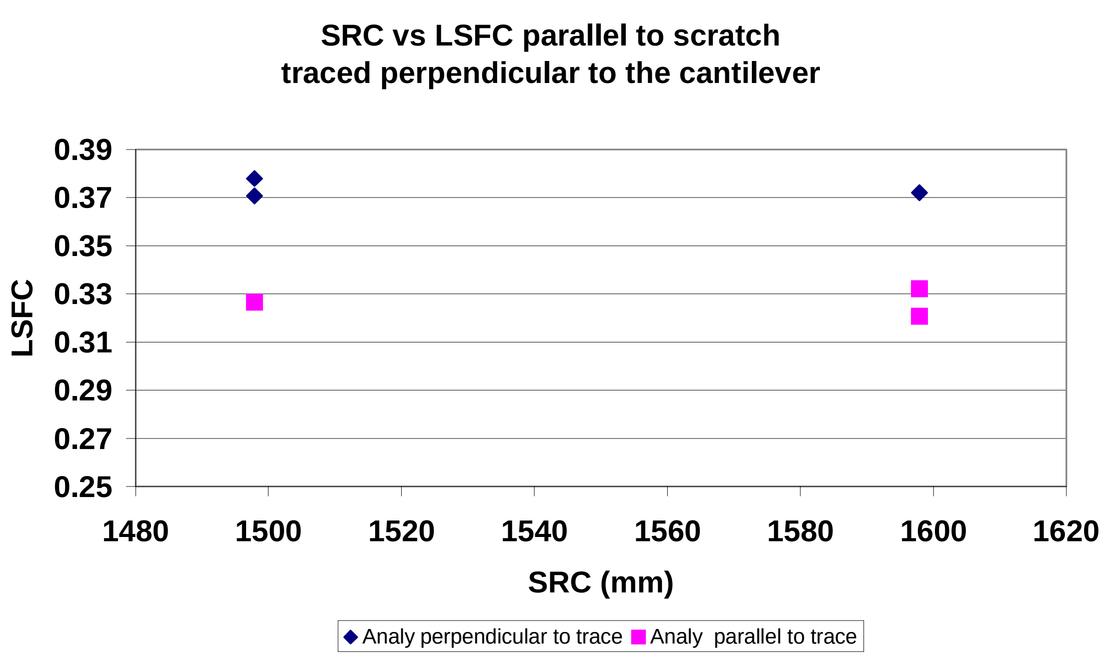

Figure 2-15 Length scale complexity vs smooth rough crossover for analysis parallel to the scratch traced at 90 deg relative to the cantilever on contact lens

2.4. Discussion

Comparison of Figure 2-5 and Figure 2-6, AFM images of the diamond coated silicone substrate at locations 1 and 2 respectively, clearly show that there is distortion of the measurements at location one assuming that the surface is indeed isotropic. The diamonds appear to be stretched out or elongated for all of the measurements at location 1. These measurements were all made by tracing in a direction at some angle other than 0° or 90° relative to the cantilever direction (see Table 2-2).

Fractal analysis shows that the measured surfaces are indeed anisotropic, as for any isotropic surface, the profile fractal dimension, for any profile taken from the surface, plus one should equal the area fractal dimension. (Russ 1994). This means that for any isotropic surface the profile fractal dimensions for any two profiles taken form the surface should be equal. Table 2-9 shows that the fractal dimensions calculated perpendicular to the tracing directions for all of the measured surfaces is higher that the fractal dimensions calculated in the tracing directions. This is a clear indication that the measured surfaces are all anisotropic.

The conventional parameters calculated do not clearly show that measurement artifacts are systematically introduced by the AFM. Looking at Figure 2-7 and Figure 2-10, the results of the conventional analysis for the two surfaces measured, there is no clear pattern that shows the analysis direction relative to the tracing direction has any affect. Figure 2-7 does show that the Pp and Pt values were always higher for the analysis in the analyses perpendicular to the tracing direction, but these differences do not seem to be statistically significant. Figure 2-10 shows that the real anisotropy of the surface masks this affect completely.

There can be a systemic difference in the smooth-rough crossover and the complexity of the profiles evaluated in the tracing and scanning directions in some situations on AFMs. This is evident by examining Figure 2-8, which shows the length scale complexity for the measurements of the diamond coated silicon substrate. Both the SRC, and Lsfc values for these measurements can be used to differentiate the analysis direction relative to the tracing direction. This difference could obscure the evaluation of the directional character of the surface, since the determination of anisotropy requires profiles to be formed in many directions on the surface.

Figure 2-11, the length scale SRC versus complexity plot shows that real anisotropy in the surface masks this effect. This plot shows the same distinction as Figure 2-8 except that the direction of the analysis relative to the scratch is what is differentiated. For this reason further comparisons should be made controlling for any possible real anisotropy in the surface. To do this it is necessary to compare only analysis made in the same direction relative to the surface.

Figure 2-8, Figure 2-12, Figure 2-13, Figure 2-14, and Figure 2-15 show that for an isotropic surface, or when the known anisotropy of a surface is controlled for, the orientation of the trace relative to the microscope is changed the difference between the relative lengths calculated from each measurement increases clearly as the scale of analysis decreases.

These figures also demonstrate that whether a surface is isotropic or anisotropic the SRC is always higher parallel to the tracing direction, and whether a surface is isotropic or anisotropic the Lsfc is always higher perpendicular to the tracing direction as long as real anisotropy in the surface is controlled for.

2.5. Conclusions

- There is clear distortion in the measured surface when the measurement is made by tracing in a direction not parallel or perpendicular to the cantilever orientation
- Conventional parameters do not clearly show that measurement artifacts are systematically introduced by the AFM.
- There can be a systemic difference in the smooth-rough crossover and the complexity of the profiles evaluated in the tracing and scanning directions in some situations on AFMs.
- Whether a surface is isotropic or anisotropic the SRC is always higher parallel to the tracing direction if any real anisotropy in the surface is controlled for.
- Whether a surface is isotropic or anisotropic the Lsfc is always higher perpendicular to the tracing direction if any real anisotropy in the surface is controlled for.

Chapter 3 SLM

3.1. Introduction

3.1.1. Objective

The objective of this chapter is to determine if measurement artifacts are systematically introduced into measured surfaces by the scanning laser microscope.

3.1.2. Rationale

Measurements made with the scanning laser microscope in the surface metrology lab at WPI have been used to predict runway friction. Friction is a directional phenomenon and anisotropy introduced by the instrument could skew the results of such a study. Additionally in measuring a strongly isotropic surface, as most manufactured surfaces are (Russ 1994), it may be possible to orient the surface in such a way as to minimize the affect of the measurement artifacts if the nature of the artifacts is understood.

3.1.3. State-of-the-art

No reference was found in the literature on study of anisotropic measurement artifacts. In 1995 William Johnsen completed an in depth study on the SLM used in this study, but did not consider the possibility of anisotropic artifacts (Johnsen 1995).

Studies on finding and characterizing anisotropy have been conducted using AFM measurements (Thomas, 1998). The SLM uses a similar method for measuring surfaces as the AFM so SLM data could also be used in such a study.

3.1.4. Approach

The approach of this chapter is similar to that of the previous chapter except that conventional roughness parameters are not considered. The fractal complexity and smooth rough crossovers calculated parallel and perpendicular to the tracing directions are compared while controlling for any real anisotropy in the surface.

3.2. Methods

This study can be broken up into two basic parts, the acquisition of the measured surfaces and the analysis of the measured surfaces.

This section of the report will describe the methods for the measurement or acquisition of the measured surfaces and the methods for the subsequent analysis of the measured surfaces.

3.2.1. Measurement

The SLM was configured to measure the surface by tracing and scanning the surface under the height sensor. The tracing tables were aligned with the plane of the sensor (Figure 1-2). The surface used was a concrete test surface that has exhibited properties of high friction and low wear (Johnsen 1997).

A 10 mm by 10 mm area was measured sampling at every 25 μm in both the tracing and scanning directions. 12 measurements were made tracing parallel to the plane of the sensor. Then 12 measurements were made tracing perpendicular to the plane of the sensor. The surface was rotated 90 degrees and an additional 12 measurements were made parallel and perpendicular to the plane of the sensor, for a total of 48 measurements. All of the measurements were made of the same 10 mm by 10 mm area. Figure 3-1 shows the SLM measuring the surface.

Figure 3-1 SLM measuring surface.

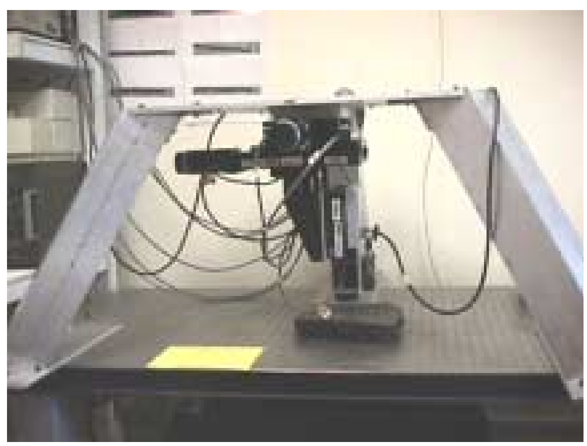

Figure 3-2 Alternate configuration of SLM.

Figure 3-2 shows the configuration of the SLM when the measurements for Johnsen 1997 were made. In this configuration the surface was fixed, and the height sensor was traced and scanned over the area to be measured. The configuration shown in Figure 3-1 was used for this study because it was supposed that there would be a smaller chance for mechanical vibrations of the height sensor due to the scanning and tracing motions, especially the acceleration and deceleration at the start and stop of each trace.

3.2.2. Analysis

Table 3-1 shows the fractal parameters calculated. (See Figure 2-3, Figure 2-4, and the description in Chapter 2 for a description of how each is calculated.

Table 3-1 Fractal surface parameters calculated for SLM study.

Profile Parameters	
Parallel to Tracing Direction	Perpendicular to Tracing Direction
Lsfc	Lsfc
SRC	SRC
Dls	Dls

As with the strongly anisotropic surface studied in Chapter 2 any real anisotropy in the surface was controlled for by only comparing analyses along the same surface direction.

3.3. Results

In this section of the report the results of the study on the SLM is reported. First the SLM images are presented. Then the results for the analysis are presented.

Figure 3-3 shows typical 10 by 10 mm images of the surface measured with the SLM..

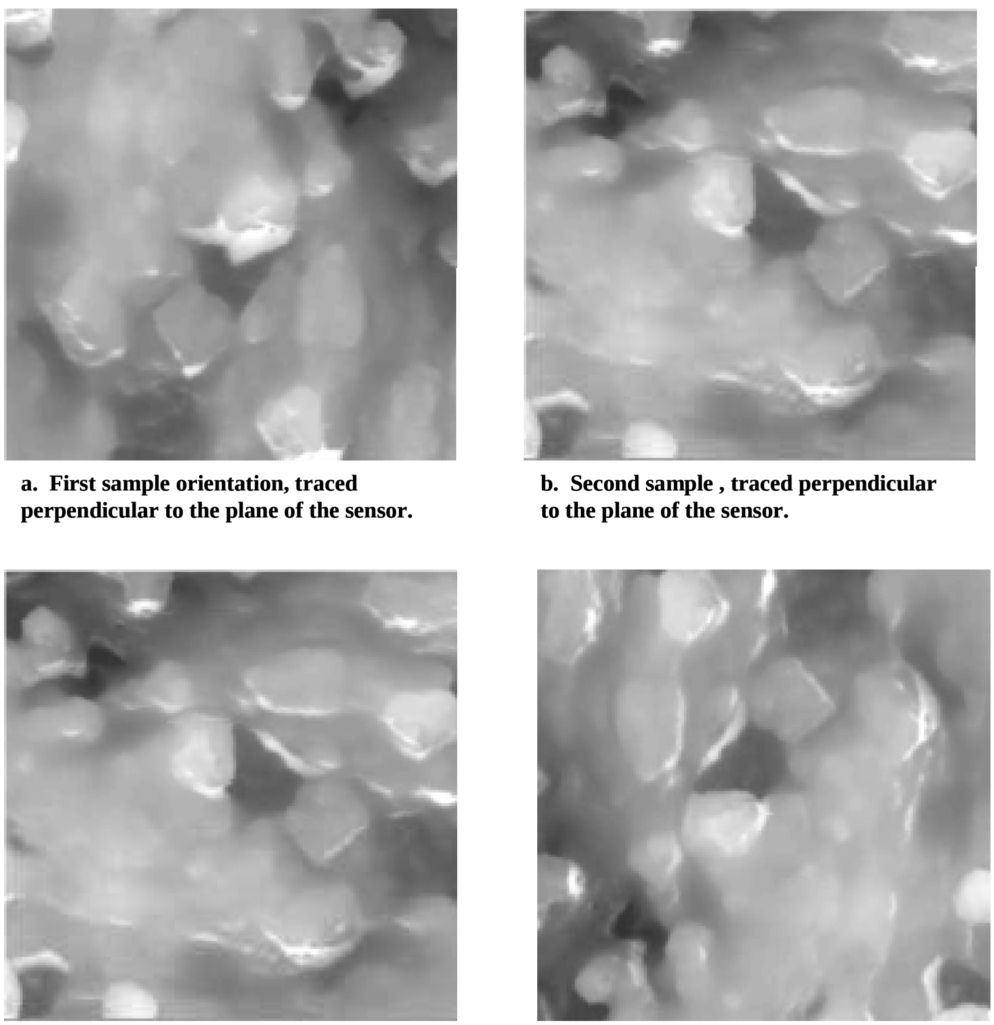

a. First sample orientation, traced perpendicular to the plane of the sensor.

b. Second sample , traced perpendicular to the plane of the sensor.

c. First sample orientation, traced parallel to the plane of the sensor.

d. Second sample orientation, traced parallel to the plane of the sensor.

Figure 3-3 Typical SLM Images of concrete surface.

3.3.1.1. Analysis

Figure 3-4shows the Lsfc vs SRC for all of the analysis of the SLM measurements. Figure 3-4 and Figure 3-5 show the same data points but separately for each analysis direction relative to the surface.

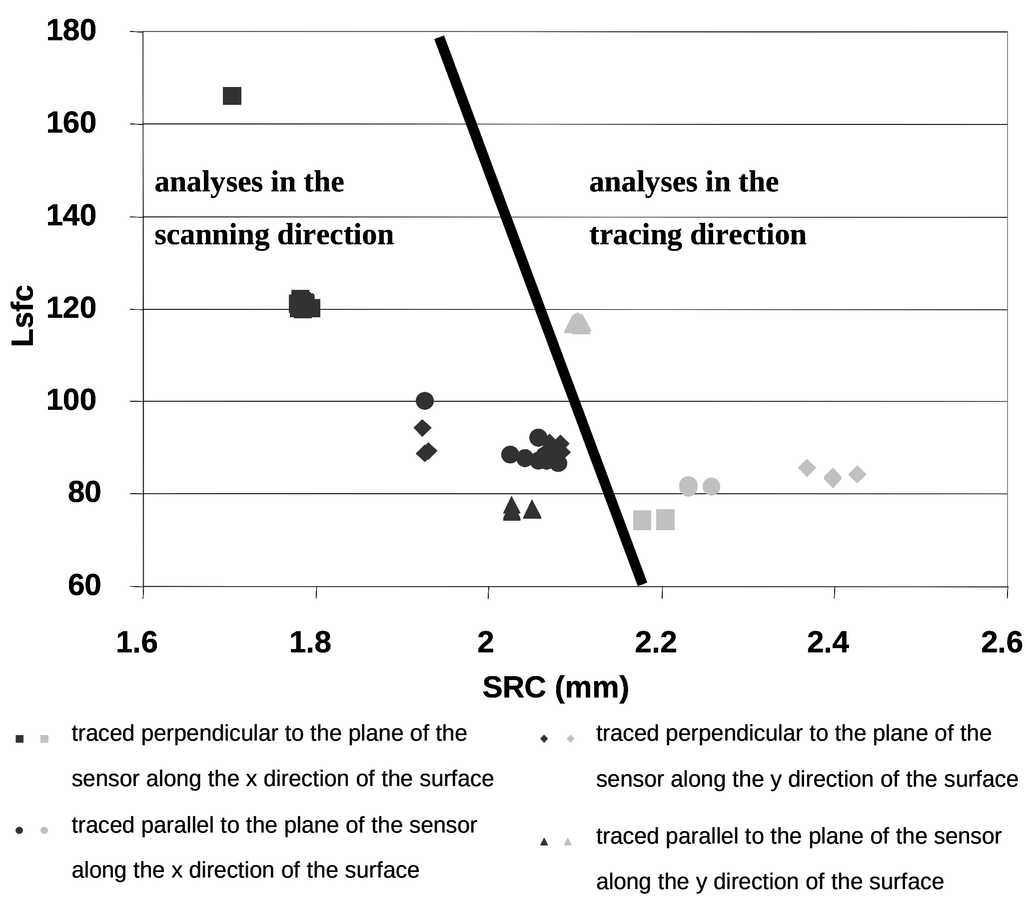

Figure 3-4 Length scale complexity vs smooth rough crossover for all SLM measurments

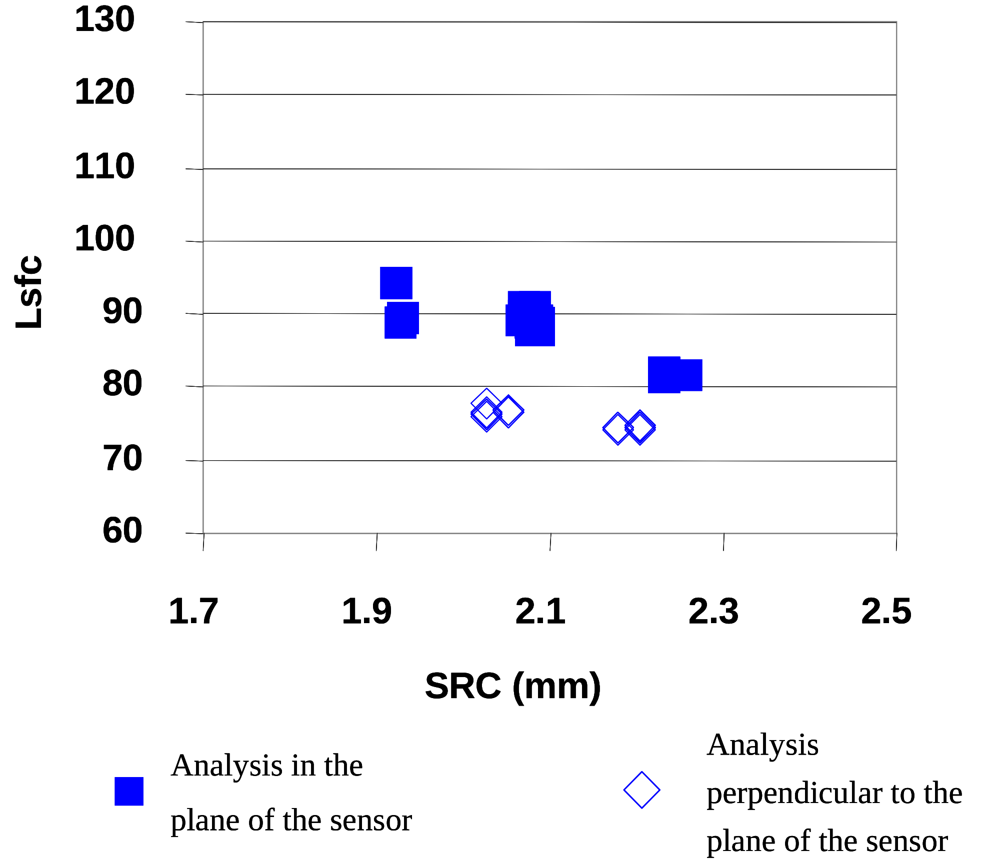

Figure 3-5 Length scale complexity vs smooth rough crossover for SLM measurments analyzed in the x direction relitive to the surface

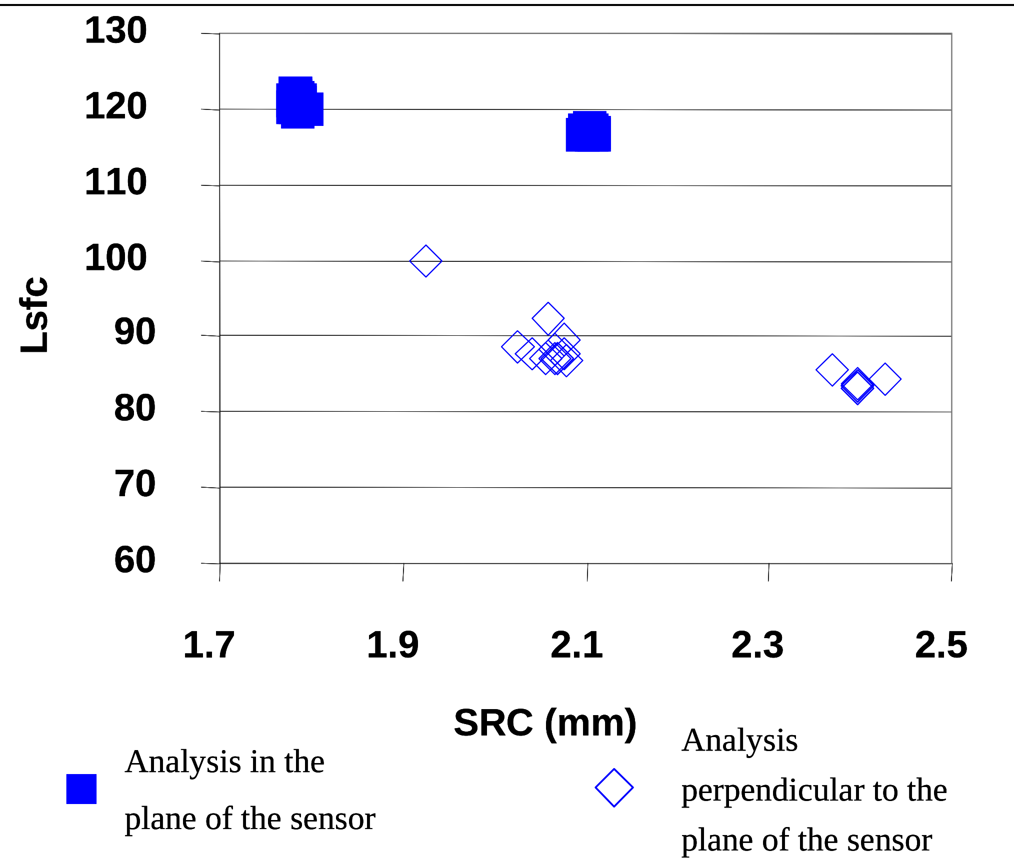

Figure 3-6 Length scale complexity vs smooth rough crossover for SLM measurments analyzed in the x direction relitive to the surface

3.4. Discussion

The plot of complexity (Lsfc) versus smooth-rough crossover (SRC) shows seven distinct different groups of results (Figure 3-4). There are only two cases where the scatter from the 12 measurements overlaps. This overlapping of the two cases is supposed to be a random event and is not considered to be consequential.

The measurements within one case appear to be highly reproducible, yet when viewed in the complexity-SRC plane it appears that the results are sensitive to all the measurement variables, sensor orientation, tracing direction, and analysis direction.

Assuming the surface is anisotropic and the complexity-SRC combination is not sensitive to the measurement variables, there would be two groups of four cases each, according to the direction of the analysis relative to the surface. This was not observed.

Instead, when controlling for any real anisotropy in the surface as discussed in Chapter 2 it can be seen that eight distinct groupings of parameters are found (see Figure 3-5). It is important to note that as with the AFM measurements of the contact lens, the anisotropic characteristics with respect to complexity are apparent, only when the orientation of the sensor is controlled. This is evident by examining Figure 3-4 and Figure 3-5. Also evident from examination of these figures is that analysis in the tracing direction results in a greater smooth-rough crossover.

The plots of SRC versus complexity can be used to differentiate sensor orientation, tracing direction and analysis direction on the same surface as long as the real anisotropy of the surface is controlled for.

An other interesting point is that analyses perpendicular to the tracing direction results in a greater scatter in the complexity of the measurements. This is evident when examining Figure 3-4 and Figure 3-5.

From these analyses it is clear that artifacts are imparted both by the orientation of the triangulation laser sensor and by the scanning and tracing tables or some noise that varies with time.

3.5. Conclusions

- The complexity - SRC space can be used to differentiate sensor orientation, tracing direction and analysis direction on the same surface.
- Anisotropic characteristics with respect to complexity are apparent, only when the orientation of the sensor is controlled.
- Analyses perpendicular to the tracing direction results in a greater scatter in the complexity of the measurements.
- Analysis in the tracing direction results in a greater smooth-rough crossover.
- Artifacts are imparted both by the orientation of the triangulation laser sensor and by the scanning and tracing tables or some noise which varies with time.

Chapter 4 Scale-sensitive analysis

4.1. Introduction

The previous two chapters have shown that for two of the three instruments examined anisotropic measurement artifacts are introduced into measured surfaces by the instruments, and it is presumed that the third instrument likewise introduced anisotropic artifacts into the measured surfaces. In this chapter, a scale based method for determining the scales over which the measurement systems are introducing anisotropy into the measured surfaces is presented and discussed.

4.1.1. Objective

The objective of this chapter is to develop a method capable of discovering the scale ranges of the anisotropic artifacts introduced by the measurement systems, and to test that method with the data from the previous two chapters.

4.1.2. Rationale

It is important to understand the scales affected by the anisotropy introduced into the measured surfaces by the instruments in order to help determine the significance of the artifacts, and to help decide if a particular instrument is a wise choice for a particular measurement task.

If, for example, the relative-length, or relative-area, at a given scale is found to be a good predictor of some physical phenomenon, and measurement artifacts cause an apparent increase or decrease from the actual relative-length or relative-area at that scale it is possible to assume that good parts could be rejected or bad parts could be accepted if the measurements were being used as part of a quality assurance inspection.

4.1.3. State-of-the-art

No method capable of discovering the scale ranges of the anisotropic artifacts introduced by the measurement systems can be found in the literature.

Scale determination and scale-based correlations are first presented by Siegmann and Brown relating to the determination of the scales over which bonds are taking place in thermal spray operations (Siegmann and Brown 2001). Further work was done by Malchiodi investigating the fracture energy versus surface area of polycrystalline graphite fracture. (Malchiodi, 2000)

4.1.4. Approach

The approach taken is similar to the scale based comparisons presented by Siegmann and Malchiodi, but in this case in stead of plotting the r-squared value of the relative lengths to some dependant variable, here the difference between the relative lengths over the entire range of scales calculated for each of the independent situations that can be considered. This difference in relative length can be plotted versus scale for each individual situation and the scale at which there begins to be a significant difference can be examined also the scale where there is a maximum difference can be seen.

As with the earlier analysis presented in chapters 2 and 3 it is necessary to control for any real anisotropy in the surface by only comparing analysis along the same direction on the surface. The other variables then such as the tracing direction, the surface orientation, and the analysis direction can them be examined one at a time.

4.2. Methods

To develop this scale determination method the measurements and analysis of the contact lens first presented in Chapter 2 are considered.

First, the cases where the tracing direction relative to the cantilever can be held constant are considered. These cases were first broken down into analysis perpendicular to the scratch and analysis parallel to the scratch. These to sets of cases were further broken down by the tracing direction relative to the cantilever. This resulted in four sets of six analyses to consider see Table 4-1. The shaded areas in the table indicate the tracing was in parallel to the cantilever orientation. The un-shaded areas were for tracing perpendicular to the cantilever orientation.

Table 4-1 Analysis with tracing direction constant and analysis direction varied

Surface orientation	Tracing direction	Analysis relative to trace	Analysis relative to surface
a	0	Perpendicular	Perpendicular to scratch
b	0	Parallel	Perpendicular to scratch
a	90	Parallel	Perpendicular to scratch
b	90	Perpendicular	Perpendicular to scratch
a	0	Parallel	Parallel to scratch
b	0	Perpendicular	Parallel to scratch
a	90	Perpendicular	Parallel to scratch
b	90	Parallel	Parallel to scratch

Length scale analysis was performed for each of the instances and the results plotted on a common set of axis. Then the difference of the average relative lengths at each scale was plotted.

Similarly, this technique was used again but instead of holding the tracing direction relative to the cantilever constant, the cases where the analysis direction relative to tracing direction was the same were analyzed while the tracing direction relative to the cantilever was allowed to vary. (Table 4-2)

Table 4-2 Analysis with tracing direction varied and analysis direction constant

Surface orientation	Tracing direction	Analysis relative to trace	Analysis relative to surface
a	0	Perpendicular	Perpendicular to scratch
b	90	Perpendicular	Perpendicular to scratch
b	0	Parallel	Perpendicular to scratch
a	90	Parallel	Perpendicular to scratch
b	0	Perpendicular	Parallel to scratch
a	90	Perpendicular	Parallel to scratch
a	0	Parallel	Parallel to scratch
b	90	Parallel	Parallel to scratch

The shaded areas in Table 4-2 indicate the analysis was perpendicular to the tracing direction.

4.3. Results

Figure 4-1 shows the length-scale plots for all analysis where the measurement was made tracing parallel to the cantilever orientation and the analysis were parallel to the scratch on the surface. Figure 4-2 shows the mean values of the two groups from Figure 4-1 plotted, and Figure 4-3 shows the difference of the relative lengths shown in Figure 4-2.

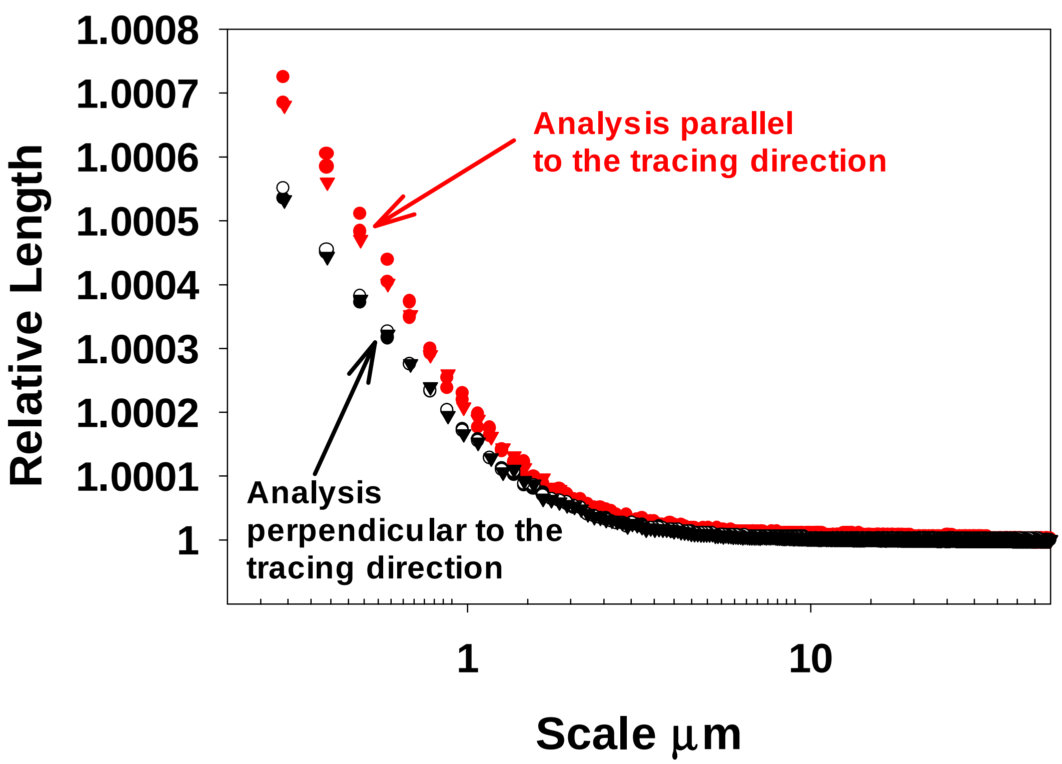

Figure 4-1 Length-scale analysis of contact lens traced at 0o to the cantilever orientation analysis parallel to the scratch

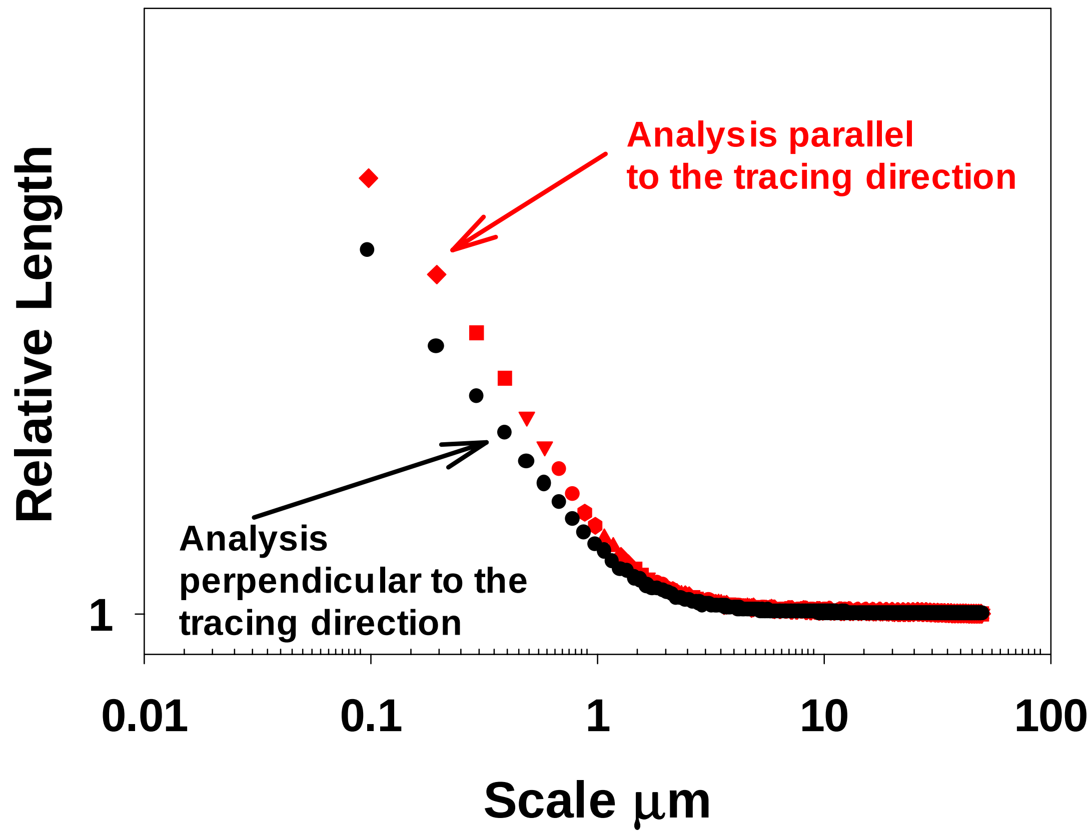

Figure 4-2 Mean length-scale analysis of contact lens traced at 0o to the cantilever orientation analysis parallel to the scratch

The same analysis was carried out for the other cases where the tracing direction relative to the cantilever was held constant and the cases where the tracing direction relative to the cantilever orientation was varied, and the analysis relative to the tracing direction was held constant showing similar results.

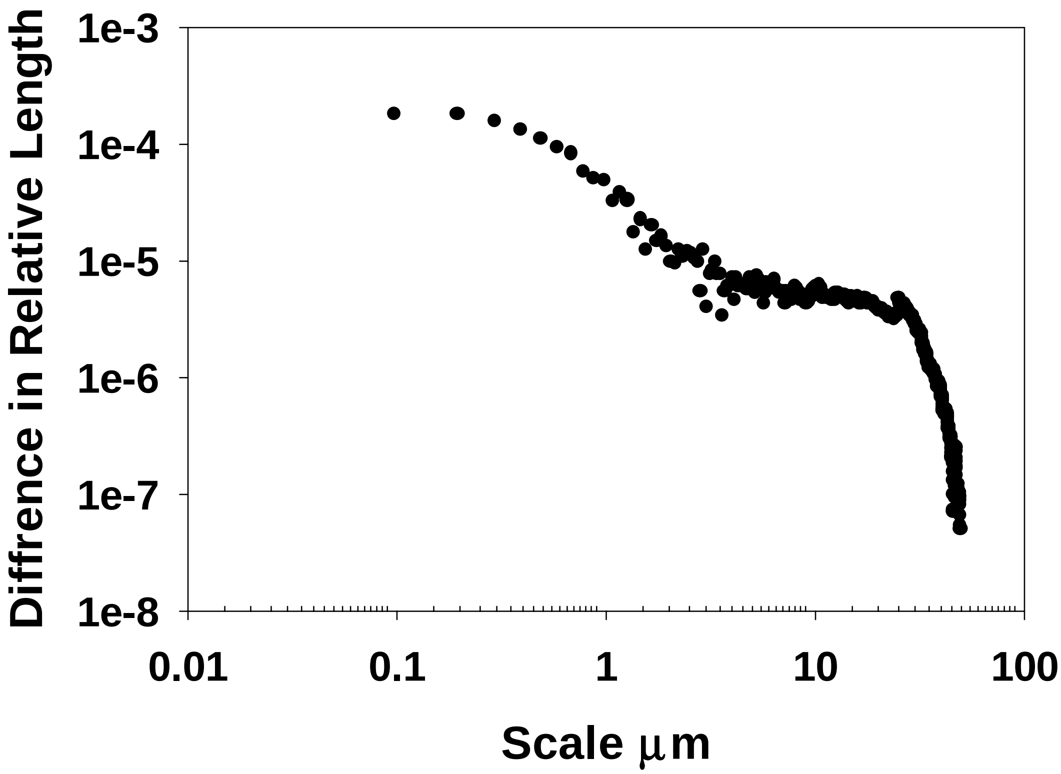

Figure 4-3 Difference of length-scale analysis of contact lens traced at 0o to the cantilever orientation analysis parallel to the scratch

4.4. Discussion

In three of the four cases where the tracing direction relative to the tip was held constant and the analysis direction relative to the tracing direction (tip) was varied the largest difference in relative area introduces was in the range of scales from 0.1μm to 1μm and the relative areas for the analysis parallel to the tracing direction were greater.

In the fourth instance however, the relative areas for the analysis perpendicular to the tracing direction were higher and there was no apparent maximum. There is possibly a change in slope at 0.11 μm but no clear drop in the difference that was exhibited in the other three instances

4.5. Conclusions

- This method can be used to determine the range of scales over which the measurement system is introducing anisotropy.
- When the orientation of the trace relative to the microscope is changed the difference between the relative lengths calculated from each measurement increases clearly as the scale of analysis decreases.

References

1. Brown, C. A., and Savary, G., "Describing Ground Surface Texture using Contact Profilometry and Fractal Analysis" Wear 141 (1991) 211-226.

2. Brown, C. A., Charles, P. D., Johnsen, W. A., Chesters, S., "Fractal Analysis of Topographic Data by the Patchwork Method", Wear 161, 61-67 (1993)

3. Bush, A. W., Gibson, R. D., and Keogh, G. P., "Strongly Anisotropic Rough Surfaces", Trans. ASME: J. Lub. Tech., 101F, 15-20 (1979)

4. Grigoriv, A. Y.,Chizhik, S. A., Myshkin, N. K., "Texture Clasification of Engineering Surfaces With Nanoscale Roughness", Trans. 7th. Int. Conf, On Metrology and Properties of Engineering Surfaces, 319-324 (Göteborg, 1997)

5. Johnsen, W. A., Design and analysis of a device to acquire detailed topographic information from pavement surfaces, Masters Thesis, Worcester Polytechnic Institute, 1995

6. Johnsen, W. A., Advances in the Design of Pavement Surfaces, Ph. D. Dissertation, Worcester Polytechnic Institute, 1997

   Malchiodi, M. C., Scale Sensitive Fractal Analysis Applied to Polychrystaline Graphite Fracture, Masters Thesis, Worcester Polytechnic Institute, 2000

7. Howland, R. and Benatar, L., "A practical Guide to Scanning Probe Microscopy", Park Scientific Instruments, (1996)

8. Russ, J. C., "Fractal Surfaces", Plenum Press, (New York, 1994)

9. Siegmann, S. and Brown, C. A., Fundamental scales of adhesion and area-scale fractal analysis, International journal of machine tools & manufacture. 41, no. 13-14, pp 1927-1933, Pergamon, (2001)

10 Thomas, T. T., "Rough Surfaces Second Edition", Imperial College Press, (1999)

11 Thomas, T.R., Rosen, B.-G., and Amini, N., "Fractal Characterization of the Anisotropy of Rough Surfaces" Wear Volume 223, 41-50, Elsevier, (1999)

12 Zahouani, H., Variolu, R., Kapsa, Ph, Loubet, J. L., and Mathia, T. G., "Effect of Lateral Resolution on Topographic Images and Three-dimensional Functional Parameters", Wear Volume 219, 114-123, Elsevier, (1998)